

Dually responsive gold-iron oxide heterodimers: merging stimuli-responsive surface properties to intrinsic inorganic material features

Hamilton Kakwere,[†] Maria-Elena Materia,[†] Alberto Curcio, [†] Mirko Prato,[†] Ayyappan Sathya,[†] Simone Nitti[†] and Teresa Pellegrino^{*†}

[†] *Istituto Italiano di Tecnologia, via Morego 30, 16145, Genoa, Italy*

*Corresponding Author *E-mail: teresa.pellegrino@iit.it*

SUPPORTING INFORMATION

Table of Contents

1. 1. Characterization Equipment.....	S3
1.1 Nuclear Magnetic Resonance (NMR) (Organic compounds characterization)	S3
1.2 Size exclusion chromatography (SEC)	S3
1.3 Dynamic Light scattering (DLS)	S3
1.4 Zeta potential	S3
1.5 Transmission electron microscopy (TEM)	S4
1.6 Turbidimetric analysis	S4
1.7 TGA analysis	S4
1.8 Elemental analysis	S4
1.9 Dynamic Scanning Calorimetry (DSC)	S4
1.10 Fluorescence spectrometry.....	S4
1.11 Magnetic characterization	S5
1.12 X-Ray Diffraction	S5
1.13 T ₁ and T ₂ time domain NMR relaxivity.....	S5
1.14 X-ray Photoelectron Spectroscopy (XPS)	S6
2. Characterization results.....	S7
2.1 Polymerization of NIPAAM and copolymerization of NIPAAM/PEGA by RAFT polymerization	S7
2.2 Determination of the LCST of PNIPAAM and PNIPAAM-co-PEGA polymers via turbidimetric analysis.....	S8
2.3 Hydrazinolysis of polymers synthesised by RAFT polymerization	S9
2.4 Functionalization of PNIPAAM-Au-Fe _x O _y -SETLRPIN nanoparticles with PDMAEA polymer	S10
2.4.1 TGA analysis	S10
2.4.2 XPS analysis	S11

2.5 X-Ray Diffraction of water transferred Au-Fe _x O _y HSs versus standard patterns of Fe _x O _y and Au	S12
2.6 TGA of Control SET-LRP reaction	S13
2.7 TEM Characterization of heterostructures.....	S14
2.8 DLS analysis of PDMAEA(Fe)-PNIPAAm-co-PEGA(Au) functionalized heterostructures below and above the pKa of PDMAEA	S16
2.9 Hydrolytic degradation of PDMAEA in water	S20
2.10 Biocompatibility assay	S20
2.11 Magnetic properties	S21
2.12 NMR measurements (Heterostructures characterization, T ₁ and T ₂ time domain) ..	S24
3. References	S25

1. Characterization Equipment

1.1 Nuclear Magnetic Resonance (NMR) (Organic compounds characterization)

NMR analyses were done using Bruker Ultra Shield Avance spectrometers 400 MHz. For all NMR analyses, unless stated otherwise, deuterated chloroform (CDCl_3) was used as the solvent with tetramethylsilane (TMS) as the internal standard.

1.2 Size exclusion chromatography (SEC)

SEC was used to determine the molecular weight of the polymers. SEC analyses were carried out at 60 °C using an Agilent SEC system equipped with a guard column and two Agilent PolarGel M columns (molecular weight range of 500-2 000 000 g/mol) attached to a differential refractive index (DRI) detector. The flow rate of the system was set at 1 mL/min and the eluent was DMF with 0.3% (w/v) LiBr. The SEC system was calibrated using Agilent narrow molecular weight distribution polystyrene standards (Varian).

1.3 Dynamic Light scattering (DLS)

Particle size measurements were carried out by dynamic light scattering (DLS) using a Malvern Instruments Zetasizer nano series instrument. An equilibration time of 3 minutes was allowed before each measurement and at least three replicate measurements were made for each sample ($[\text{Fe}] = \text{ca. } 25 \text{ ppm}$).

1.4 Zeta potential

Zeta potential measurements were carried out using a Malvern Instruments Nano ZS90 (Malvern, USA) at 25 °C equipped with a 4.0 mW He-Ne laser operating at 633 nm and an avalanche photodiode detector. The sample was placed in a plastic folded capillary cell (0.75 mL). An equilibration time of 3 minutes was allowed before each measurement and at least five replicated measurements were made for each sample ($[\text{Fe}] = \text{ca. } 25 \text{ ppm}$). Measurements at different pH values were carried out in the pH range 3-11 and before each zeta potential measurement, pH adjustments were done using HCl (1M) or NaOH (1M) while the pH was monitored using a calibrated Crison Basic 20 pH meter at 37 °C using the above-mentioned equilibration and measurement parameters.

1.5 Transmission electron microscopy (TEM)

TEM images were obtained using JEOL JEM 1011 electron microscope with acceleration voltage of 100 kV. Samples were prepared by placing a drop of sample onto a carbon coated copper grid which was then left to dry before imaging.

1.6 Turbidimetric analysis

Turbidimetric analyses were done using a Varian Cary 5000 UV-vis spectrophotometer equipped with Peltier elements for temperature control. Measurements were done on solutions of 1 mg/mL of PNIPAAm polymer and before each measurement, the sample (ca. 3 mL) was placed in a quartz cuvette (1cm × 1cm) left to equilibrate at the desired temperature for 3 minutes.

1.7 TGA analysis

The weight loss of the functionalised nanoparticles was determined by using a TA Instruments Hi-Res TGA 2950 thermogravimetric analyzer under a nitrogen atmosphere (60 cm³/min). The samples (2-3 mg as total mass) were heated from room temperature to 95 °C at a heating rate of 10 °C/min and isothermal for 15 min then to 600 °C .

1.8 Elemental analysis

To measure Fe, Sulphur and Gold ratio, elemental analysis was carried out by means of an Inductively Coupled Plasma (ICP) Atomic Emission Spectroscopy on a ThermoFisher CAP 6000 series. The samples were prepared by digesting 25 µL of sample in 2 mL of aqua regia overnight followed by dilution with MilliQ water to 25 mL.

1.9 Dynamic Scanning Calorimetry (DSC)

DSC measurements were conducted using a Perkin Elmer diamond DSC calibrated using an indium metal standard. The heating rate from 5 to 80 °C was 1 °C/min and the temperature was held constant at the low temperature (5 °C) for 10 minutes before measurement.

1.10 Fluorescence spectrometry

Fluorescence spectroscopy measurements were done using a Varian Cary fluorescence spectrophotometer in a quartz cuvette with a path length of 1 cm using ca. 3 mL of sample.

1.11 Magnetic characterization

Magnetic characterization was carried out by using a superconducting quantum interference device (SQUID) from Quantum Design. Hysteresis curves were measured from -70 to + 70 kOe at 5 K and 298 K. Temperature dependent magnetization studies, zero field cool (ZFC) and field cool (FC) curves were recorded in the range of 4 to 300 K. The FC measurements were performed under a magnetic field of 50 Oe. The known concentration of 50 μ L is dropped on top of the Teflon tap, after the sample get dried out, the sample was load for measurements.

1.12 X-Ray Diffraction

XRD measurements were performed on a Rigaku SmartLab X-ray diffractometer operating at 40 kV and 150 mA. The diffractometer was equipped with Cu source and a Gobel mirror in order to have a parallel beam and it was used in 2-theta/omega scan geometry for the acquisition of the data. Specimens for XRD measurement were prepared by dropping, 200 μ L of a concentrated solution of dimers onto a zero background silicon substrate.

1.13 T_1 and T_2 time domain NMR relaxivity

The longitudinal (T_1) and transverse (T_2) relaxation times are measured using a Minispec spectrometer (Bruker, Germany) mq 20 (0.5 T), mq 40 (1 T) and mq 60 (1.5 T). The T_1 relaxation profile was obtained using an inversion–recovery sequence, with 20 data points and 4 acquisitions for each measurement. T_2 relaxation time was measured using a Carr–Purcell Meiboom Gill (CPMG) spin–echo pulse sequence with 200 data points with inter echo time of 0.5 ms. The relaxivities r_i ($i = 1, 2$) are determined from the slop of the following equation:

$$\frac{1}{T_{i(Obs)}} = \frac{1}{T_{i(H_2O)}} + r_i C_{Fe} \quad (i = 1, 2)$$

where, C_{Fe} is the concentration of Fe ions. The values are reproducible within 5% deviation.

Samples of polymer coated HSs at concentrations between 0.25 mM (Fe) and 0.75 mM (Fe) were prepared in pork skin gel (0.5%). The desired amount of nanoparticles from a stock solution of THF was transferred into a dry glass vial using a micropipette and the THF was removed using a stream argon followed by the addition of a known volume of water. The nanoparticles were dispersed via sonication for 30 seconds at 10 °C and the amount of pork skin gel required to obtain a concentration of 0.5% was then added from a stock solution.

Samples were mixed thoroughly using a micropipette and transferred into NMR tubes which were placed at 0 °C for 30 minutes before measurement.

1.14 X-ray Photoelectron Spectroscopy (XPS)

The XPS analyses were carried out with a Kratos Axis Ultra spectrometer using a monochromatic Al K(alpha) source (20mA, 15kV). Samples were prepared by drop casting of few μL of the HSs solution (ca. 1.5 mg/mL of Fe in THF or chloroform) on highly oriented pyrolytic graphite (HOPG, ZYB grade) substrates. The Kratos charge neutralizer system was used on all samples. Survey scan analyses were carried out with an analysis area of 300 x 700 microns and a pass energy of 160 eV. High resolution analyses were carried out on the same analysis area at pass energy of 10 eV and step of 0.1 eV. The photoelectrons were detected at a take-off angle of $\Phi = 0^\circ$ with respect to the surface normal. The pressure in the analysis chamber was maintained below 7×10^{-9} Torr for data acquisition. Spectra have been charge corrected to the main line of the C 1s spectrum set to 284.8 eV (C-C bonds). Spectra were analysed using CasaXPS software (version 2.3.16).

2. Characterization results

2.1 Polymerization of NIPAAM and copolymerization of NIPAAM/PEGA by RAFT polymerization

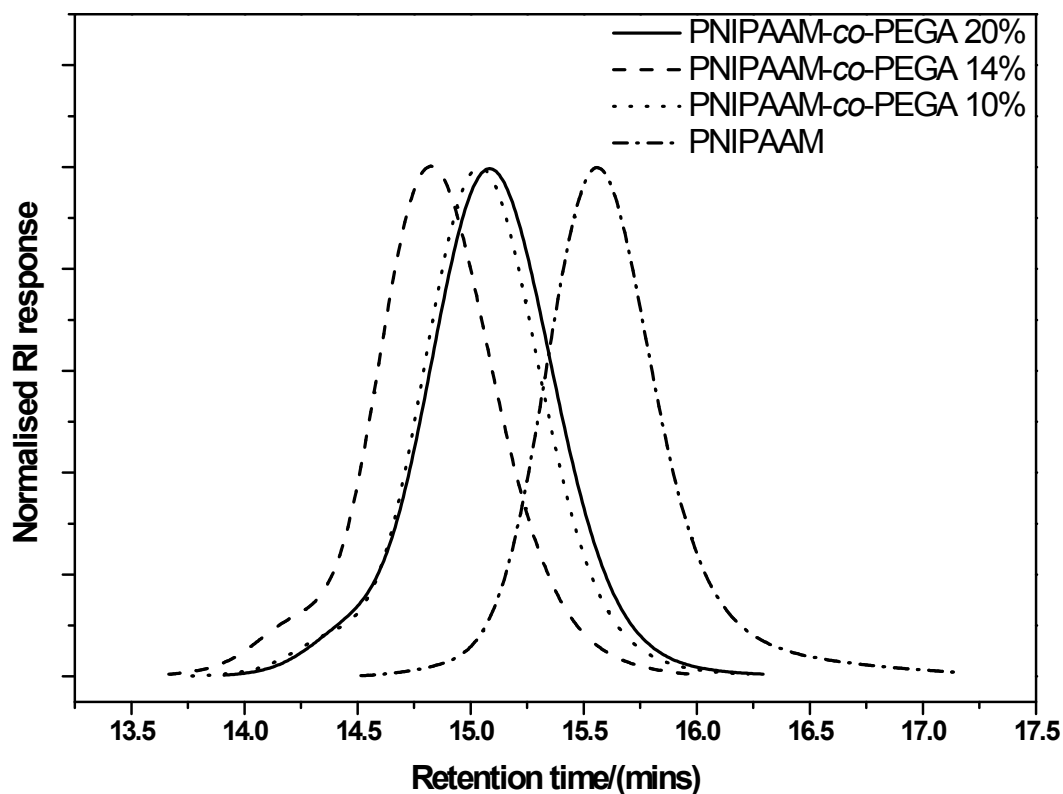


Figure S1: SEC chromatograms for PNIPAAm and PNIPAAm-*co*-PEGA copolymers. The percentage shown is the mol% of PEGA used during polymerization (feed composition) with the remaining percentage being NIPAAM. PNIPAAm ($M_n = 7600$ g/mol , $PDI = 1.2$), PNIPAAm-*co*-PEGA 10% ($M_n = 8700$ g/mol , $PDI = 1.2$), PNIPAAm-*co*-PEGA 14% ($M_n = 10200$ g/mol, $PDI = 1.2$) and PNIPAAm-*co*-PEGA 20% ($M_n = 8600$, $PDI = 1.2$).

2.2 Determination of the LCST of PNIPAAm and PNIPAAm-*co*-PEGA polymers via turbidimetric analysis

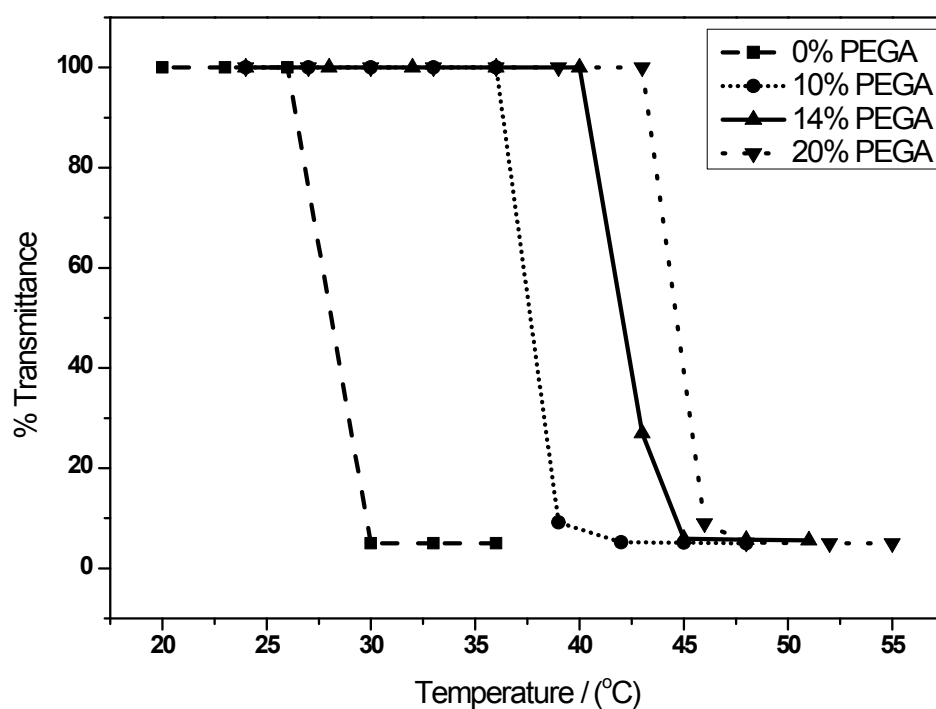


Figure S2: LCST determination via turbidimetric measurements of solutions of PNIPAAm and PNIPAAm-*co*-PEGA copolymers. The percentage shown is the mol% of PEGA used during polymerization with the remaining percentage being NIPAAm.

2.3 Hydrazinolysis of polymers synthesised by RAFT polymerization

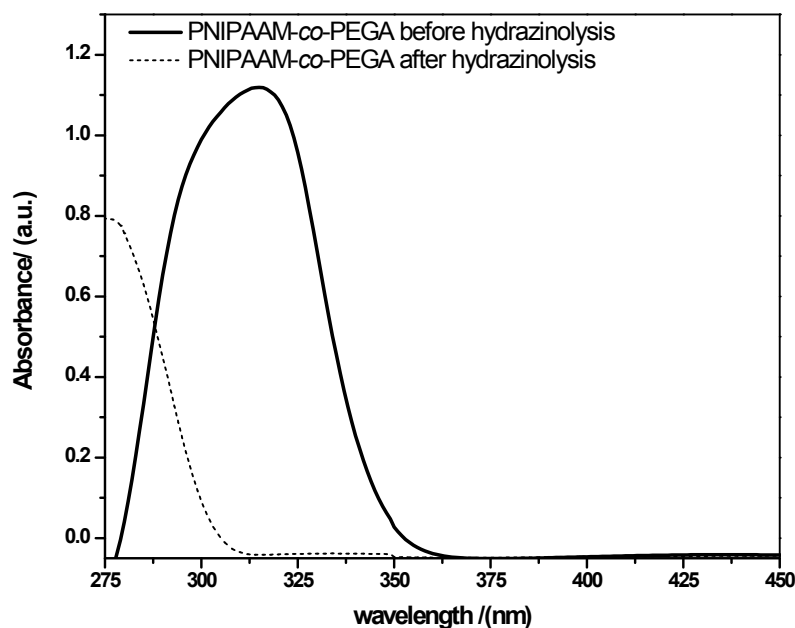


Figure S3: UV vis spectra of PNIPAAm-*co*-PEGA before and after hydrazinolysis. The absorption maximum at 306 nm is due to the trithiocarbonate of the RAFT agent which disappears upon hydrolysis.

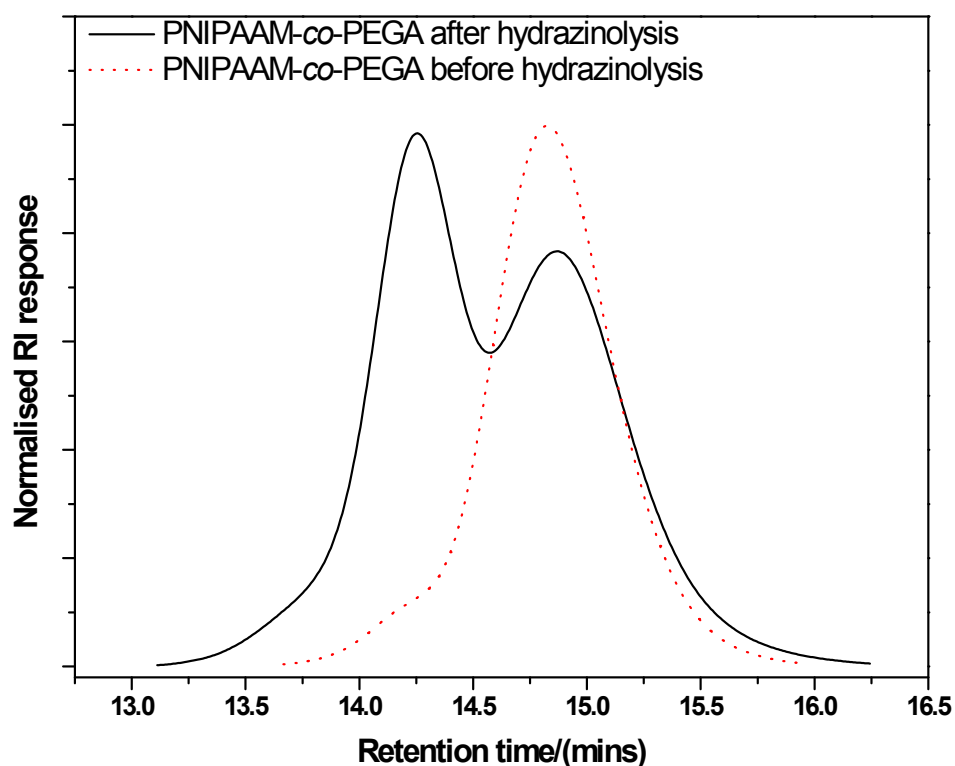


Figure S4: SEC chromatograms of PNIPAAm-*co*-PEGA before and after hydrazinolysis. Both thiol functionalized (retention time 14.9 mins, M_n 10200 g/mol) and disulfide polymers (retention time 14.1 mins, M_n 21700 g/mol) were present with some disulfides forming possibly during the analysis.

2.4 Functionalization of PNIPAAm-Au-Fe_xO_y-SETLRPIN nanoparticles with PDMAEA polymer

2.4.1 TGA analysis

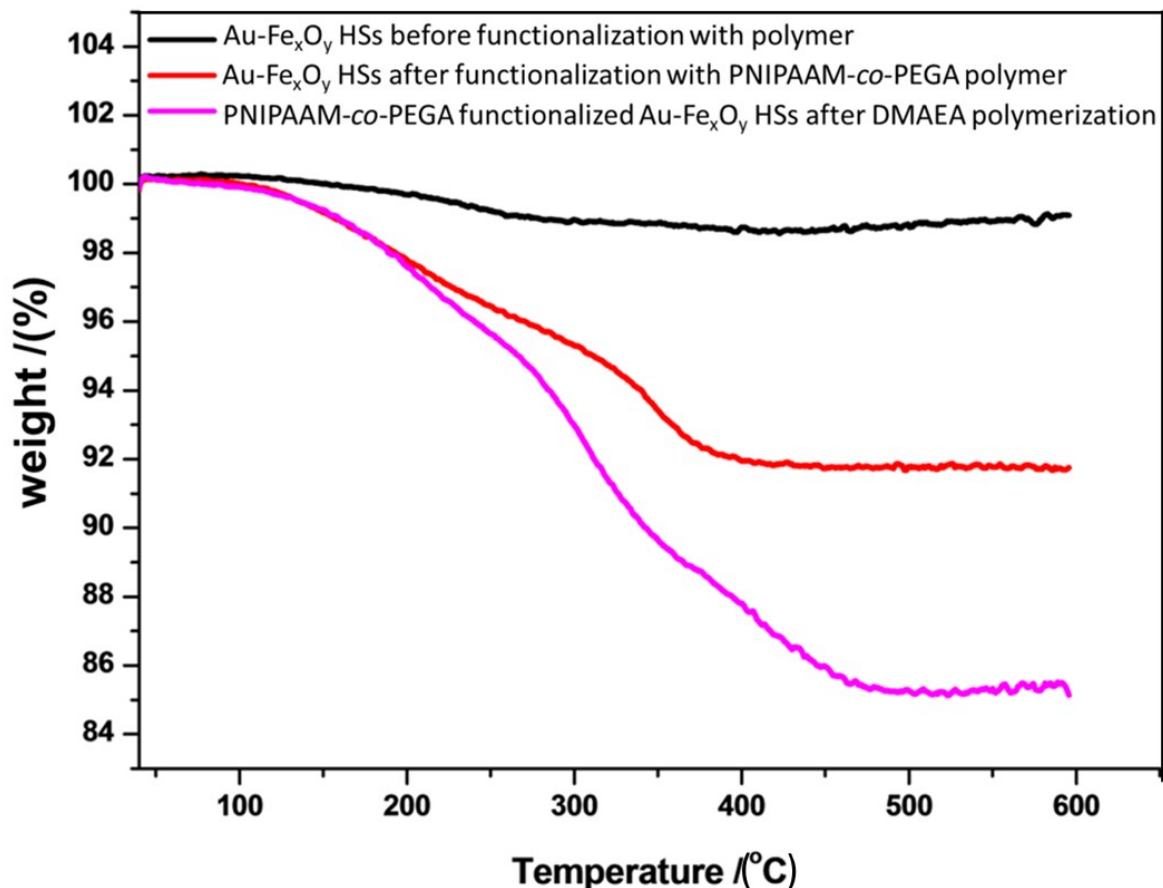


Figure S5: Weight loss determination via TGA of Au-Fe_xO_y HSs at different functionalization steps. (black curve) Before functionalization showing very little weight loss (< 1%) due to loss of short molecule ligand surfactants. (red curve) After functionalization with PNIPAAm-co-PEGA a more significant weight loss (ca. 8 %) was recorded indicating the presence of more organic material (polymer). (magenta curve) After SET-LRP using DMAEA a more pronounced weight loss (ca. 16 %) was detected as both domains of the HSs are covered with polymer.

2.4.2 XPS analysis

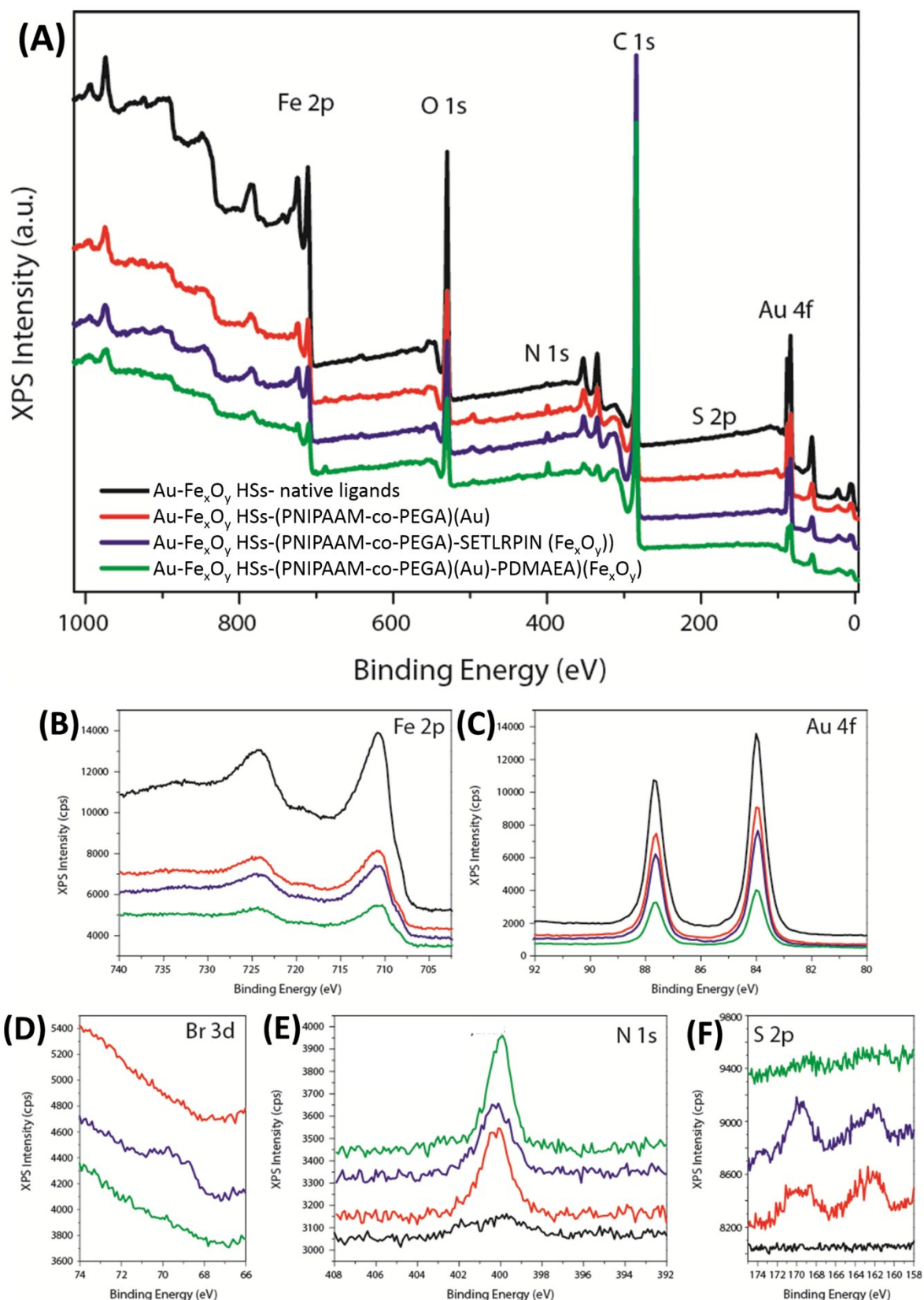


Figure S6: XPS spectra obtained for the starting Au-Fe_xO_y HSs (black), Au-Fe_xO_y HSs after the modification with PNIPAAm-co-PEGA (red), PNIPAAm-co-PEGA functionalised Au-Fe_xO_y HSs after modification with and SETLRPIN (purple) and PNIPAAm-co-PEGA/PDMAEMA functionalised Au-Fe_xO_y HSs after SET-LRP (green). The full spectrum

is shown in (A) and high resolution XPS spectra showing specific regions for different elements regions are in (B-F).

2.5 X-Ray Diffraction of water transferred Au-Fe_xO_y HSs versus standard patterns of Fe_xO_y and Au

XRD measurements were performed on a Rigaku SmartLab X-ray diffractometer operating at 40 kV and 150 mA. The diffractometer was equipped with Cu source and a Gobel mirror in order to have a parallel beam and it was used in 2-theta/omega scan geometry for the acquisition of the data. Specimens for XRD measurement were prepared by dropping 200 μ L a concentrated solution of dimers HSs onto a zero background silicon substrate.

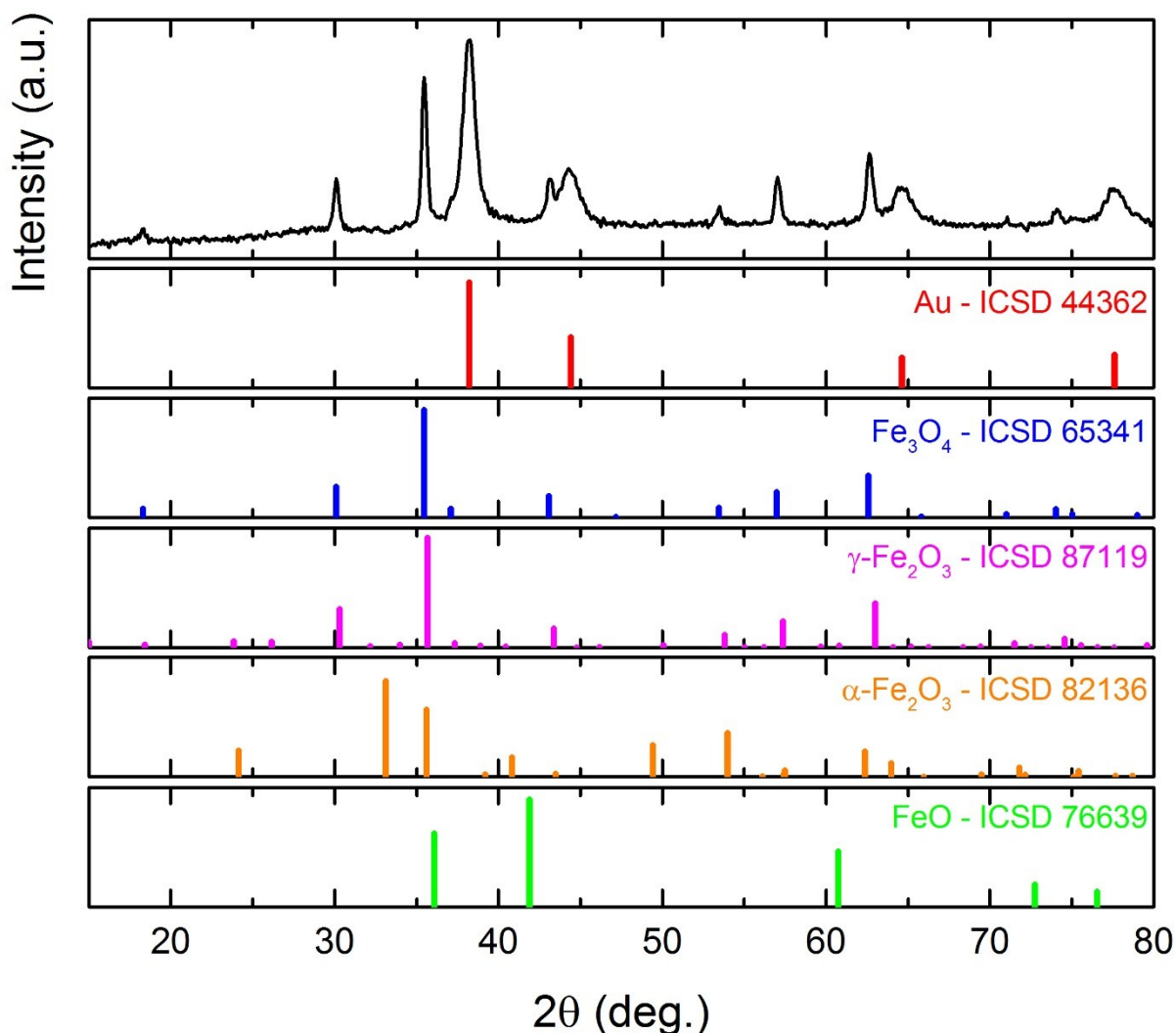


Figure S7: XRD pattern of Au-Fe_xO_y HSs sample (after polymerization) is compared with standard patterns of Au, Fe₃O₄, γ-Fe₂O₃, FeO, and α-Fe₂O₃. Even if oxidation of HSs occurs after water transfer and a possible appearance of α-Fe₂O₃ is indicated by ZFC/FC

measurements, no confirmation can be obtained by the XRD patterns as the main peak of α - Fe_2O_3 are not present in the pattern of HS. This might indicate that the fraction of α Fe_2O_3 phase in the final sample is below the detection limit of XRD (few percent).

2.6 TGA of Control SET-LRP reaction

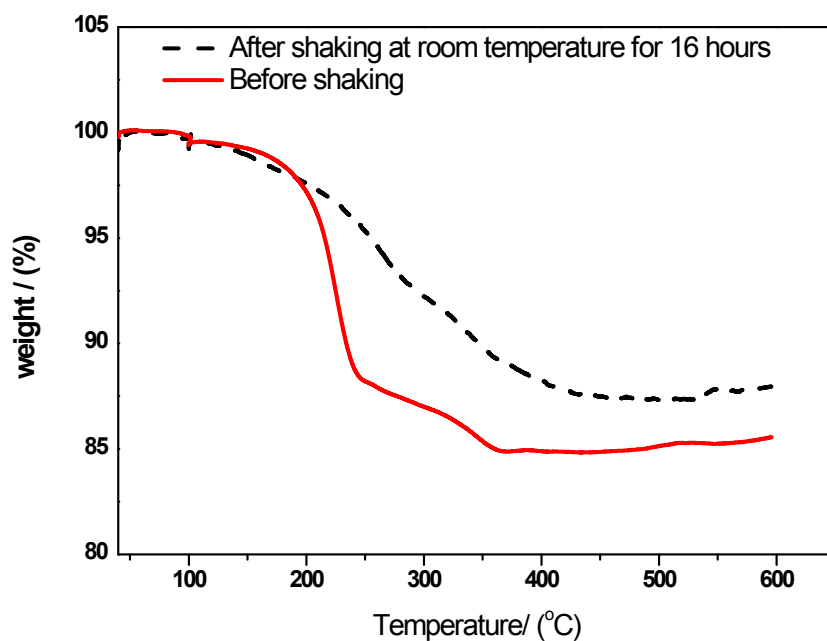


Figure S8: TGA of PNIPAAm-*co*-PEGA modified Au- Fe_xO_y HSs before and after control SET-LRP. The minor decrease in weight loss indicates most chains remain attached to the Au surface during the SET-LRP procedure.

2.7 TEM characterization of heterostructures

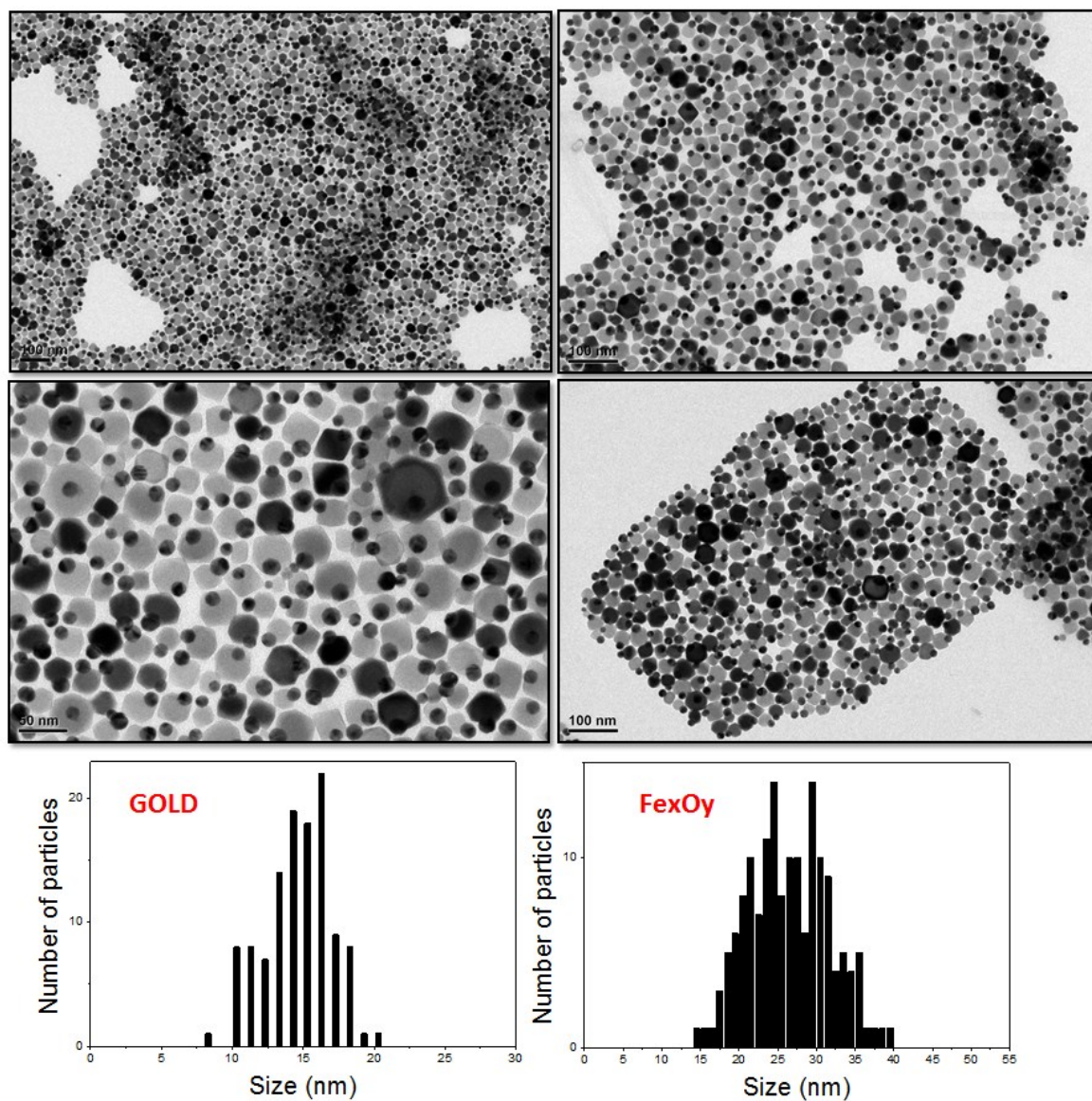


Fig. S9. A collection of TEM images of as-synthesized Au-Fe₃O₄ heterostructures deposited from a chloroform solution. Also, the statistic plot of gold and iron oxide size versus number of particles is shown. Average domain sizes have been calculated on 138 heterostructures for the gold and on 158 for the Fe₃O₄ nanoparticles respectively.

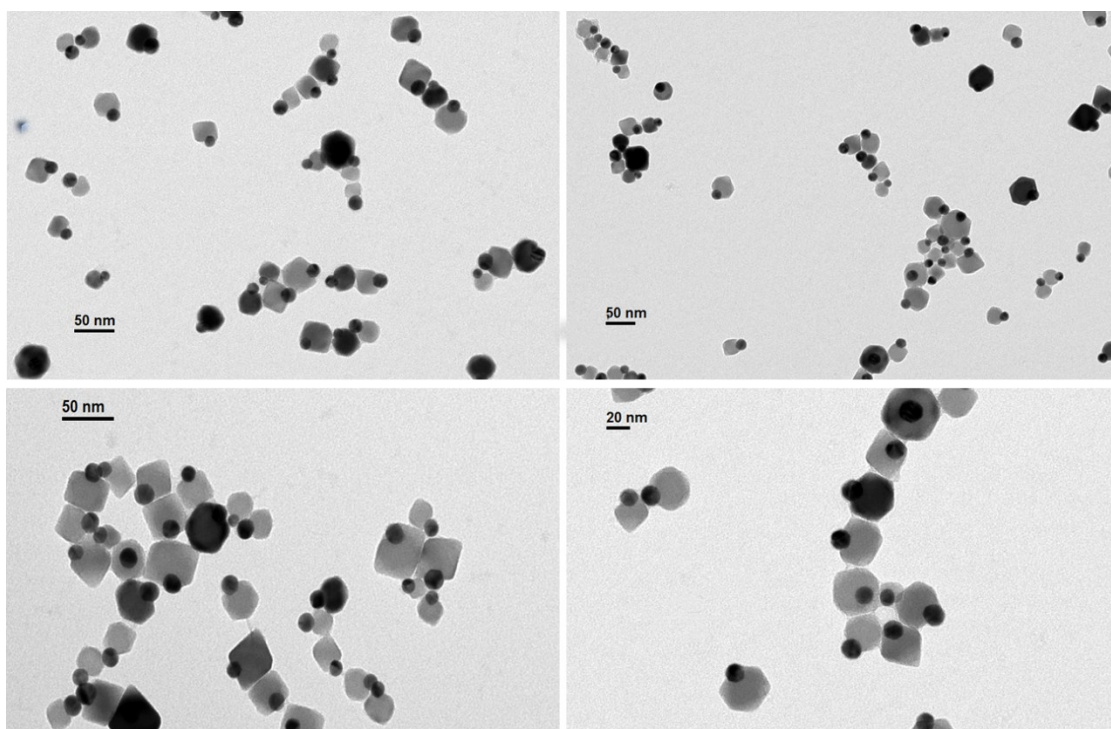


Fig. S10. A collection of TEM images of Au-FexOy heterostructures deposited from an aqueous solution after water transfer and polymer decoration.

2.8 DLS analysis of PDMAEA(Fe)-PNIPAAm-*co*-PEGA(Au) functionalized heterostructures below and above the pKa of PDMAEA

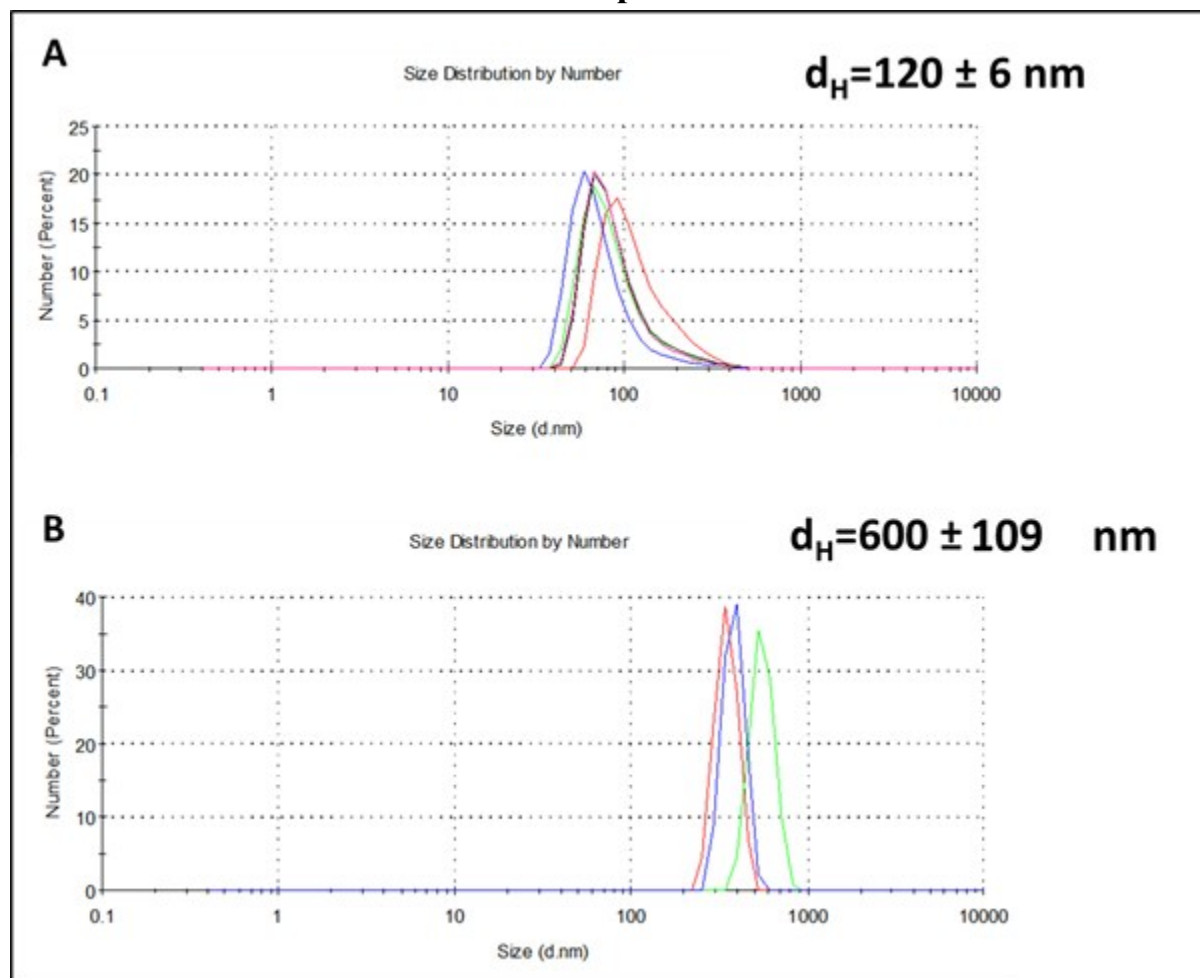


Figure S11: DLS measurements for the PDMAEA(Fe)-PNIPAAm-*co*-PEGA(Au) functionalized Au-Fe_xO_y HSs at pH 5 (A) and at pH 10 (B), that is above the pKa 8 of the PDMAEA.

2.9 Hydrolytic degradation of PDMAEA in water

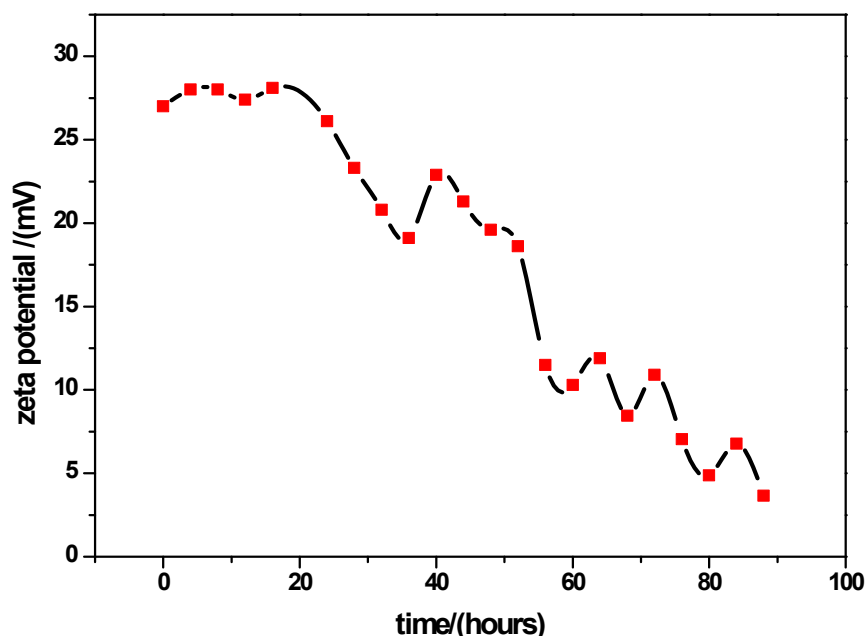


Figure S12: Variation of zeta potential with time for the polymer functionalized Au-Fe_xO_y HSs in water.

2.10 Biocompatibility assay

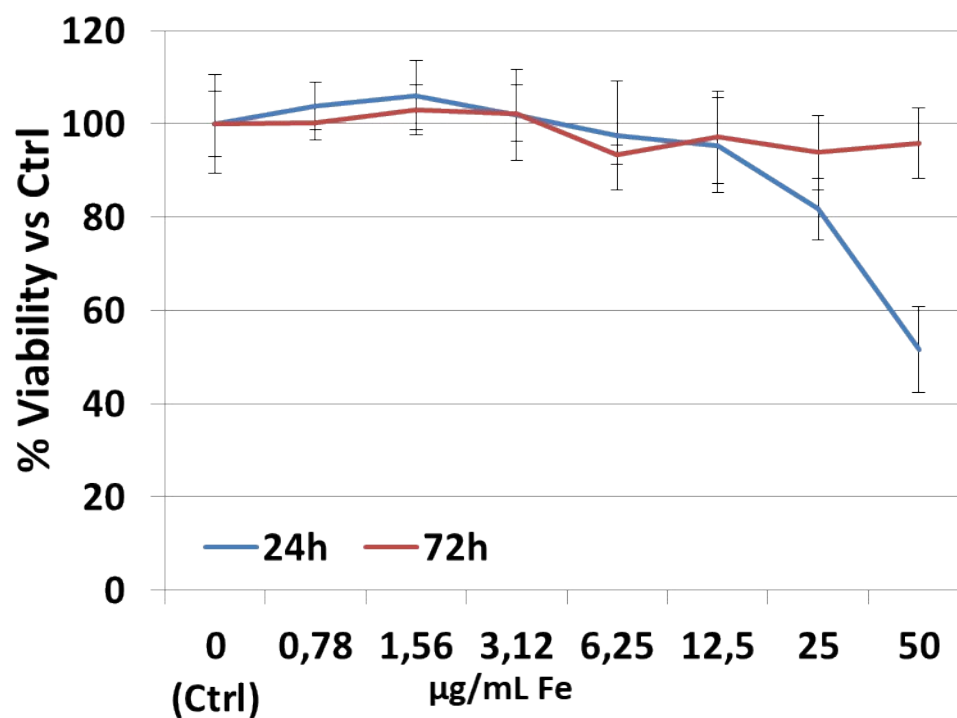


Figure S13: Viability percentage of KB cells exposed to HSs dimers at different concentrations after 24 (24h) or 24 hours of incubation plus further 48 hours with fresh media (24h + 48h).

2.11 Magnetic properties

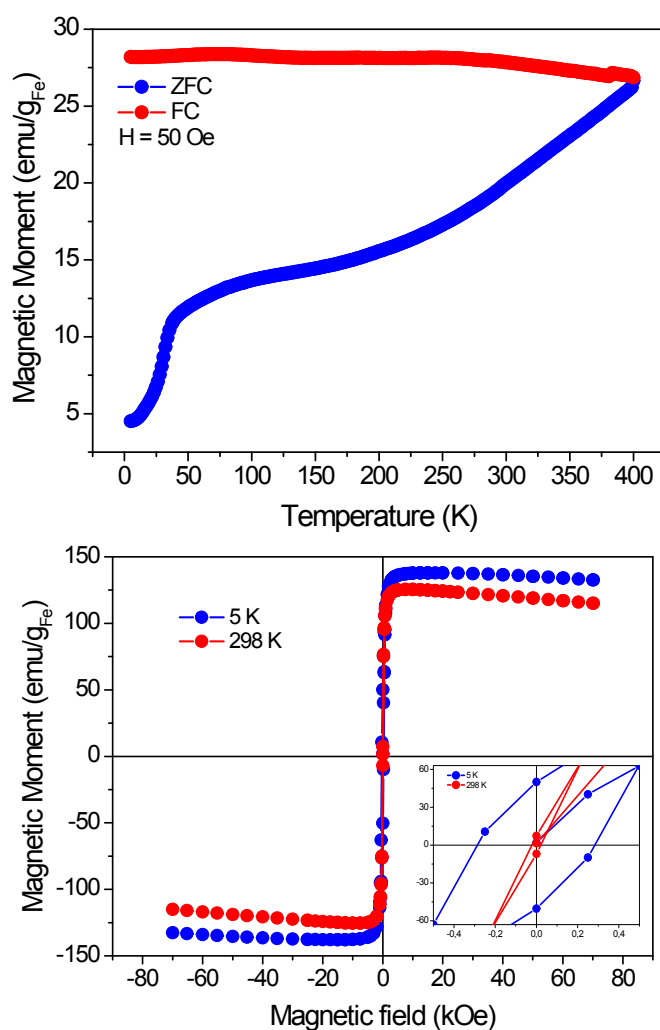
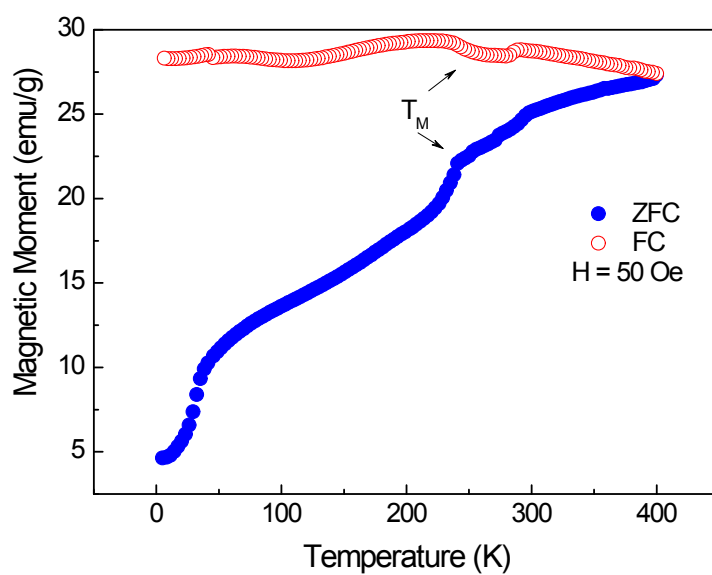


Figure S14: Temperature dependent magnetization zero field cool (ZFC) and field cool (FC) curves (upper panel) and hysteresis loops (lower panel) at 5 and 298 K for gold-iron oxide dimer NPs before functionalization with polymers. Insert shows the zoomed view.



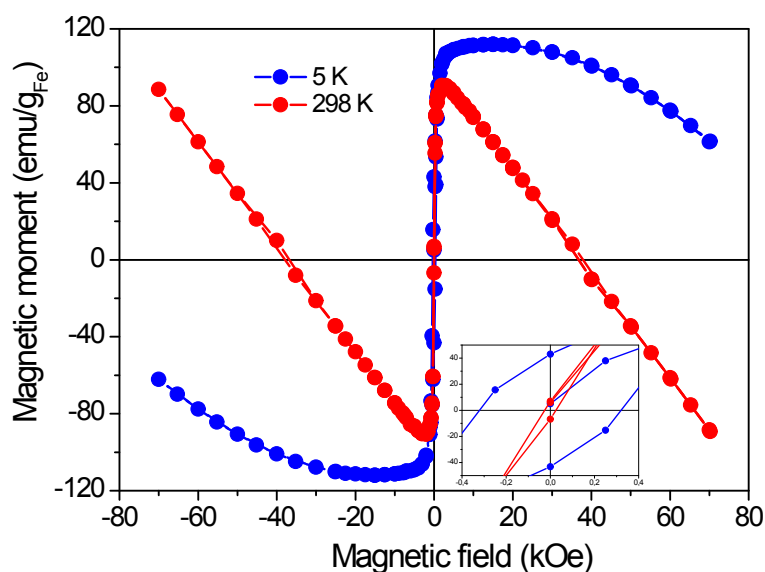


Figure S15: Temperature dependent magnetization zero field cool (ZFC) and field cool (FC) curves (upper panel) and hysteresis loops (lower panel) at 5 and 298 K for gold-iron oxide dimer NPs after functionalization with polymers on both Au and Fe_xO_y domains. Insert shows the zoomed view. A feeble kink around 240 K, observed only after water transfer, could be due to the Morin temperature (T_M) of possible α -Fe₂O₃ phase due to oxidation process occurring after polymer coating and water transfer of γ -Fe₂O₃ to α -Fe₂O₃ as previously reported.^{1, 2}

2.12 NMR measurements (Heterostructures characterization, T_1 and T_2 time domain)

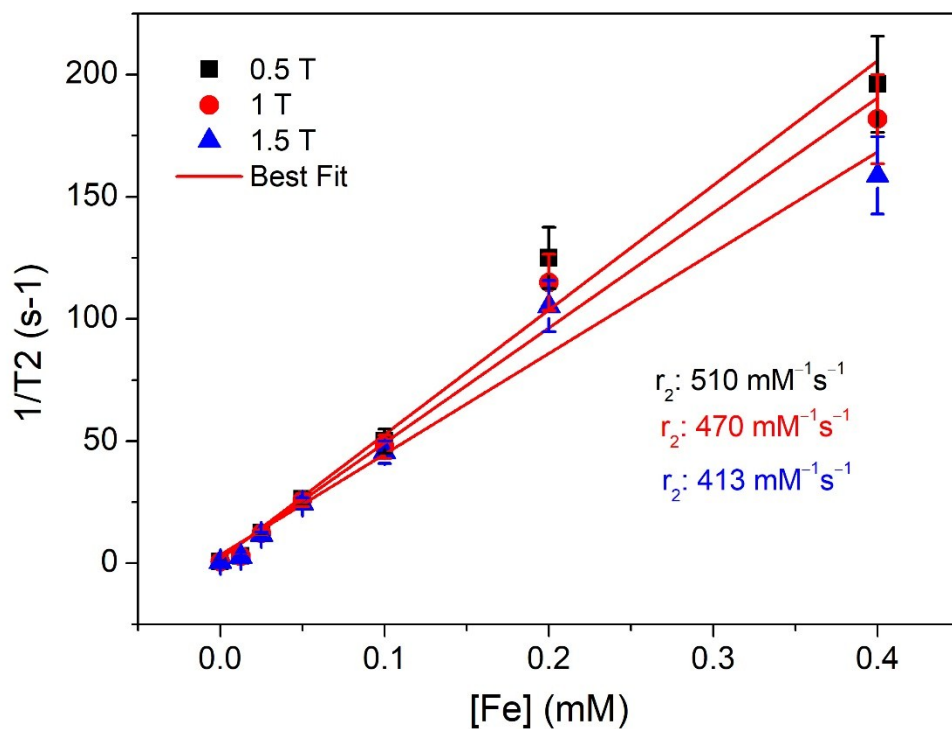


Figure S16: An inverse of T_2 (r_2) versus iron concentration of polymer functionalized (with both the thermo-responsive and pH-responsive polymers) Au-Fe HS dimers in 0.5 % pork skin gel medium at pH7.

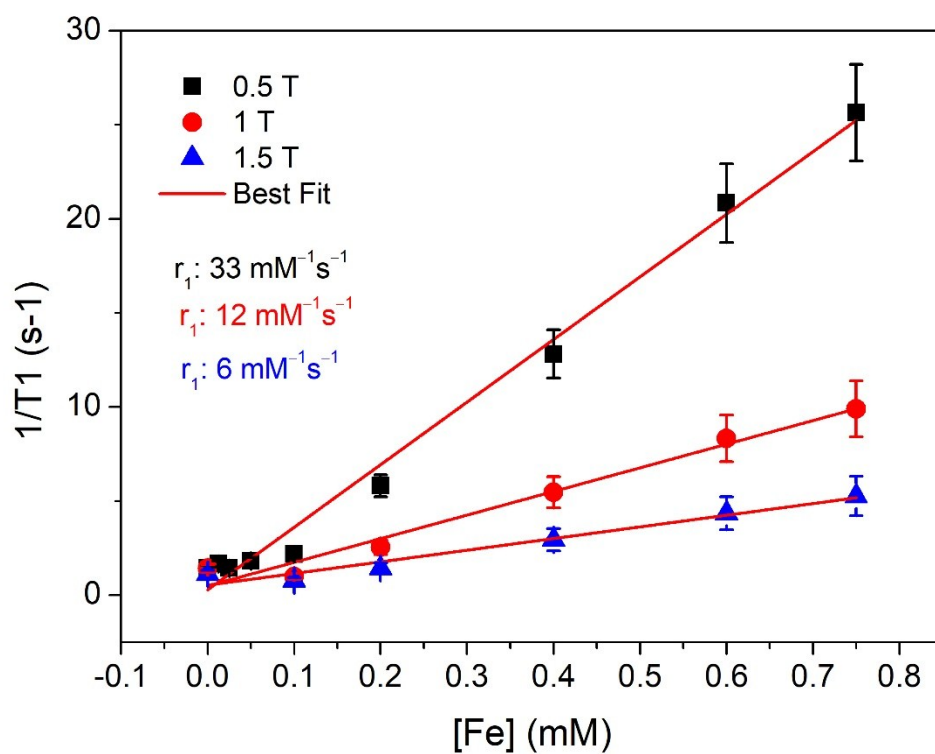


Figure S17: An inverse of T_1 (r_1) versus iron concentration of polymer functionalized (with both the thermo-responsive and pH-responsive polymers) Au-Fe_xO_y HS dimers in 0.5 % pork skin gel medium at pH 7.

3. References

1. S. Najafshirvani, T. M. Kokumai, S. Marras, P. Destro, M. Prato, A. Scarpellini, R. Brescia, A. Lak, T. Pellegrino, D. Zanchet, L. Manna and M. Colombo, *ACS Appl. Mater. Interfaces*, 2016, **8**, 28624-28632.
2. L. Machala, J. Tuček and R. Zbořil, *Chem. Mater.*, 2011, **23**, 3255-3272.